Predicting the effects of oscillator-based assistance on stride-to-stride variability of Parkinsonian walkers*

Virginie Otlet[1] and Renaud Ronsse[1]

***Abstract*— Parkinson's disease is a severe neurodegenerative disorder that affects sensorimotor control. In particular, several gait impairments are reported, including a decrease of long-range autocorrelations in stride duration time series. This complex statistics is potentially a biomarker of the risk of falling. This paper aims at developing model-based predictions about the loss of long-range autocorrelations in the gait of Parkinsonian patients, and how these autocorrelations can be restored by an oscillator-based walking assistance. Using a Super Central Pattern Generator model coupled with an adaptive oscillator, we show that this type of assistance has the potential to improve long-range autocorrelations in time series of Parkinsonian walkers. This requires however to tune the adaptive oscillator with slow learning gains, raising challenges for porting this method to an actual device.**

I. Introduction

Parkinson's disease is the second most common neurodegenerative disorder worldwide, affecting over 10 million people nowadays [1]. Patients with this disease encounter a lot of gait impairments such as decreased gait speed, stride length, and cadence, as compared to age-matched healthy individuals [2]. This leads to an increased risk of falling and affects their everyday life [3]. Indeed, the risk of falling and resulting fractures is twice as likely in Parkinsonian patients as in age-matched healthy individuals [4]. In a recent study, Warlop and colleagues [5] suggested that a particular metrics, namely the assessment of long-range autocorrelations (LRA), is a marker of the risk of falling in Parkinsonian patients, allowing to detect gait instability before the first actual fall.

Over the past decades, the assessment of LRA in series of biological signals – such as gait, heartbeat, breathing, neural activities, etc. [6] – has received increasing attention. In the particular case of walking, this feature refers to the presence of a persistent inter-dependence between the durations of consecutive strides. In other words, the duration of the current step significantly depends on all the preceding ones, including those that happened several minutes ago. It is believed that the presence of LRA in gait time series is a marker of the stability, adaptability and flexibility of the locomotor system [7]. In particular, a decrease in the presence of LRA in time series of inter-stride intervals indicates a more random temporal organization, hallmark of gait instability. Several independent studies have reported a decreased presence of LRA in the time series of Parkinsonian patients as compared to those of healthy people [5], [9], [10].

Fig. 1: The Active Pelvis Orthosis developed in the framework of the CYBERLEGsPlusPlus project [8] can deliver oscillator-based walking assistance to the user's hip. It is now brought to a commercial product by the company IUVO (Pisa, Italy, `www.iuvo.company`).

The goal of this paper is to develop a set of model-based predictions about the deterioration of LRA in people affected by Parkinson's disease, and how this can be partially restored by an assistive method mediated by a robot. Indeed, in recent years, robot-assisted gait training has received a growing interest to improve gait of Parkinsonian patients. First-generation devices were end-effector robots – such as the Gait Trainer GT1 (Reha-Stim, Berlin, Germany) [11] – or exoskeletons – such as the Lokomat (Hocoma, Zurich, Switzerland) [12] – that repeatedly applied a nominal gait pattern with high intensity to the patient [13]. This therapy has demonstrated some interesting results for patients, such as improved gait velocity, endurance, stride length and duration, cadence, and balance, and a reduction in severity and frequency of freezing of gait episodes, as summarized in [14]. Moreover, some of these improvements were maintained weeks after treatment. However, this type of robot does not allow the patient to recover a healthy inter-stride variability, because it applies a stereotyped and constant gait pattern. Moreover, it does not allow the patient to actively participate in the movement. In contrast, more

*This work was supported by the Fonds de la Recherche Scientifique - FNRS under Grant n^o PDR T.0200.19: PaDAWAn project.

[1]Virginie Otlet and Renaud Ronsse are with the Institute of Mechanics, Materials, and Civil Engineering; the Institute of Neuroscience; and Louvain Bionics, UCLouvain, 1348 Louvain-la-Neuve, Belgium `virginie.otlet@uclouvain.be`

compliant robots can increase the benefits of such therapies for patients, as was shown with other pathologies [15], [16].

There is a large body of literature that developed and validated compliant approaches for robotic locomotion therapies although, to the best of our knowledge, this has never been tested with Parkinsonian patients. In the present paper, we develop a model providing a prediction about the effect of one of these approaches in particular, regarding the presence of LRA in Parkinsonian patients. The framework that is modelled in this paper leverages on the intrinsic periodicity of locomotion and is based on so-called adaptive oscillators. An adaptive oscillator (AO) is a mathematical tool capable of learning the features of a periodic quasi-sinusoidal input signal in dedicated state variables capturing its phase, frequency, amplitude, etc [17]. This particular framework acts like a filter to smooth the input signal, and can predict the estimated signal evolution in real-time, *i.e.* without delay, based on the filtered estimation of the state variables [18]. In [19], walking assistance was delivered as an image of the difference between the estimated position in the near future and the current one, such that the user's hips were attracted towards their own predicted future. In [20], it was shown that delivering a similarly computed assistance that is proportional to the difference between the *current* estimate and the *actual* signal actually helps in smoothing the movement but with no injection of mechanical work, on average.

The actual implementation of an AO-based assistive framework has already been implemented on several actual wearable devices for the lower-limb [19], [21]–[23], on top of which the Active Pelvis Orthosis developed in the framework of the CYBERLEGsPlusPlus project (Figure 1). This device has been initially designed for transfemoral amputees, in order to assist the hip flexion-extension movement and thus to reduce the metabolic cost of walking [24]. It has already been used in several (pre)clinical investigations, that reported interesting effects on the elderly [25], such as increased gait efficiency, decreased metabolic cost, increased activation of hip extensor muscles and increased range of hip motion. Although the same benefits might be transferable to Parkinsonian patients, there is no evidence they would be correlated to changes in LRA. The main contribution of this paper is thus to provide a step towards assessing the putative effect of an AO-based assistance on the LRA of Parkinsonian patients, by means of model-based predictions.

The paper is structured as follows. Section II describes the methods to (i) model inter-stride time series containing LRA for Parkinsonian walkers, (ii) include walking assistance in this modeling framework, (iii) assess LRA in those simulated time series, and (iv) perform statistical analyses. Then Section III provides the results of these statistical tests. In Section IV, simulation results are discussed and compared to what could be obtained during real experiments. The paper ends with a conclusion.

II. Methods

In this section, we describe the model used to produce inter-stride intervals time series of Parkinsonian patients containing LRA, and how we added the effect of an assistance based on AO to this model.

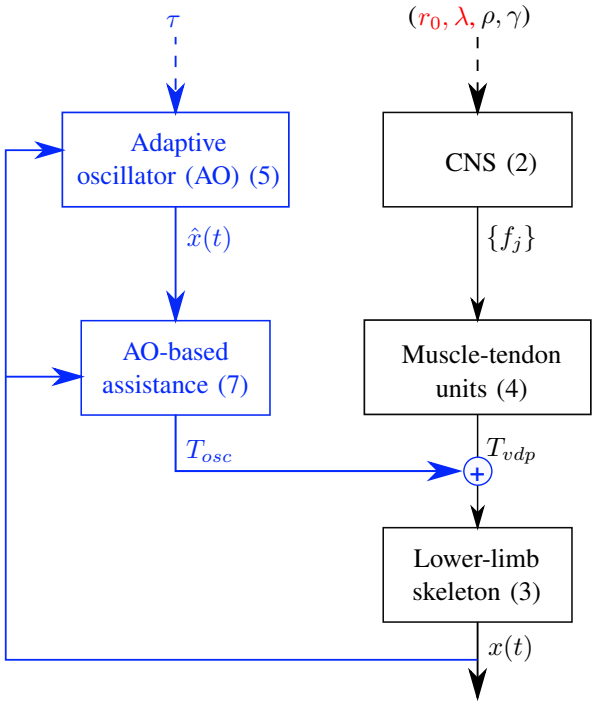

Fig. 2: Block diagram of the SCPG model and body (black) coupled to an AO-based assistance (blue). The parameters highlighted in red are those to be adapted from healthy values to take into account the impact of PD. Model parameters are indicated by dashed lines. Numerical labels refer to the corresponding equations in the text.

A. Model

1) Super Central Pattern Generator (SCPG): For this part, we adopted the same formalism as [26], [27] in order to generate inter-stride intervals time series containing LRA with similar properties as healthy human walkers.

This model is composed of two parts. The first one represents a Central Pattern Generator (CPG), modelled through a Markov chain (Figure 3). Its nodes X_i can be seen as neural centers firing at a particular action potential. These nodes are exponentially correlated, because neighbouring neurons of a CPG are likely to be influenced by similar factors. This Markov chain is thus modelled by [26], [27]:

$$X_i = \exp(-1/r_0) X_{i-1} + \varepsilon_i \quad (1)$$

with r_0 the short-range spatial correlation size, and ε a zero-centered discrete Gaussian process of variance λ^2 [27]. From this short-range correlated series $\{X_i\}$, a new long-range correlated one $\{X_j\}$ is obtained by following the

jumps of a random walker along this chain. The jump size follows a Gaussian distribution of width ρ, *i.e.* $\sim \mathcal{N}(0, \sigma^2)$ with $\sigma = \rho/\left(2\sqrt{2\ln(2)}\right)$.

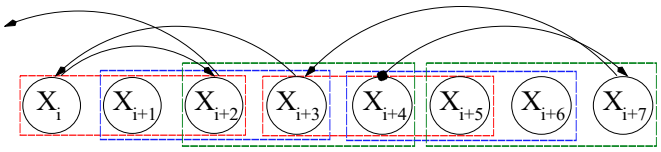

Fig. 3: Illustration of the Markov chain characterizing the CPG. The values of the action potentials X_i are short-range correlated, forming superimposed neuronal zones (dashed colored boxes) of size $r_0 = 3$ in this example, centered around each neuronal center. Arrows indicate the jumps of the random walker (adapted from [28]).

Each of these action potentials X_j are linked to a frequency, resulting in a long-range correlated time series of frequencies [26], [27]:

$$f_j = f_0 + \gamma X_j \tag{2}$$

where f_0 is the driver frequency, *i.e.* the average frequency of the series, and γ a constant.

The second part of this model captures a dynamical model of the lower-limb biomechanics. It takes the time series $\{f_j\}$ of the previous part as input to a forced van der Pol oscillator. Therefore, the j^{th} cycle of this oscillator is initiated with an intrinsic frequency f_j. The system composed of (3) and (4) forms a van der Pol oscillator, as described in [26], [27]:

$$\ddot{x} = T_{vdp} \tag{3}$$

$$T_{vdp} = \sin(2\pi f_0 t) - x^2\dot{x} + \dot{x} - (2\pi f_j)^2 x \tag{4}$$

where $x(t)$ is the hip angular position and $\dot{x}(t)$ and $\ddot{x}(t)$ represent its two first time-derivatives, *i.e.* angular velocity and acceleration of the hip. This oscillator is driven by a periodic force, characterized by a nominal frequency f_0, that is equal to the average of the frequency series of (2). The simulated inter-stride intervals time series is therefore given by the actual period of the successive cycles of $x(t)$, obtained by solving this second-order differential equation using a four-stage Runge-Kutta integrator [26]. By convention, these cycles are delimited by the zero-crossings of the signal $x(t)$ when it is decreasing.

2) Walking assistance: In this work, we assume that the walking assistance is delivered by AO. In our case, the periodic input signal is the hip angular trajectory $x(t)$, and a smoothed version of this input, $\hat{x}(t)$, can be obtained from an AO with the following equation [19]:

$$\hat{x}(t) = a_1(t)\sin(\varphi(t)) + a_0(t) \tag{5}$$

where the phase $\varphi(t)$, the frequency $\omega(t)$, the amplitude $a_1(t)$ and the offset $a_0(t)$ are learned by the internal dynamics of the AO, see (10)-(13) in the appendix. Note that the whole dynamics of the AO can be tuned by a single parameter, namely τ, that governs the learning rate of the AO state variables, see (14) in the appendix.

The device provides an assistive torque T_{osc} that is proportional to the difference between the current estimate $\hat{x}(t)$ and the actual signal $x(t)$ of the hip position, similarly to what [20] did for the upper-limb. A supplementary term is thus added to the van der Pol oscillator equation (3):

$$\ddot{x} = T_{vdp} + T_{osc} \tag{6}$$

$$T_{osc} = -k(x - \hat{x}) \tag{7}$$

where k acts as a virtual stiffness, determining the level of assistance.

In order to estimate the contribution of this extra assistance torque in the whole dynamics of the model, we computed δ_{osc} as the ratio between the peak torque provided by the assistance over the peak total torque, *i.e.*:

$$\delta_{osc} = \frac{\max_{cycle}|T_{osc}|}{\max_{cycle}|T_{vdp} + T_{osc}|} \cdot 100 \ [\%] \tag{8}$$

3) Selection of parameter values: In order to simulate time series corresponding to Parkinsonian patients, some parameters of the model have to be adapted compared to the values reported in [26], [27] for healthy people. Neurodegenerative disorders like Parkinson's disease can be interpreted in this model as a decrease in the correlation between neural centers, characterized by r_0 [26]. To match the decreased presence of LRA in real time series of Parkinsonian patients (obtained from [5]), this parameter was decreased to $r_0 = 6$ compared to the value for a healthy subject, *i.e.* $r_0 = 25$. To take into account the increased standard deviation of those time series, λ was set to 0.8, and finally, $f_0 = 1/1.07$ [Hz] since the mean stride durations for Parkinsonian patients is equal to 1.07 sec, as obtained from real time series [5]. The other parameters of the model are left at the same values as in [26], [27], *i.e.* $\gamma = 0.02$ and $\rho = 25$.

In this paper, we would like to predict the effect of the AO-based assistance for several magnitudes of assistance k and several learning time constants τ of the oscillator. We particularly explored 30 combinations, *i.e.* $k = 2, 4, ..., 20$ [N·m/deg] and $\tau = 0.5, 4, 10$ [s]. One hundred series of frequencies $\{f_j\}$ containing 1024 points each were simulated in Matlab R2019a for each pair of assistance parameters (k, τ).

B. LRA assessment

Time series containing LRA have a correlation function that decreases according to a power law [29]:

$$C(t) = Cov(y_i, y_{i+t}) \sim t^{-\beta} \tag{9}$$

with $Cov(\cdot)$ the covariance function, t the time lag between two observations of a time series y, and β the scaling

exponent which should be $0 < \beta < 1$ for a long-range correlated time series.

To assess the presence of LRA in the simulated time series, we do not assess directly this scaling exponent β, but rather the so-called Hurst exponent H, related to it by the relationship $\beta = 2H - 2$ [30]. In order to do so, the evenly spaced averaged detrended fluctuation analysis (esaDFA) is used in this article. This method – described in details in [31] – has been selected for two reasons. Firstly, DFA method can be applied to both stationary and non-stationary time series. Secondly, adding evenly spacing to this method decreases the variability obtained in the estimation of the Hurst exponent [31]. Briefly, a time series of length N is first integrated and subsequently divided into non-overlapping intervals of length n. The time series within each interval is then detrended to remove the local trend. The root-mean-square fluctuation function $F(n_i)$ is computed on each interval, then averaged over all the intervals of length n_i, so that the average magnitude of fluctuation $F(n)$ is obtained [31], [32]. This process is repeated over all interval lengths n, ranging from 10 to $N/2$. To obtain evenly spaced values of n in log scale, the range of $\log(n)$ is divided into a series of intervals of equal length, and the points falling within each interval are averaged. Finally, $\log\big(F(n)\big)$ is plotted against $\log(n)$, and the Hurst exponent is obtained by computing the slope of the regression line [31].

Although the Hurst exponent has been defined in the literature as being between 0 and 1 [33], the DFA method can lead to values larger than 1, because of its relevance for both stationary and non-stationary time series. In order to be consistent with the literature, we use the notation of the α exponent instead of the Hurst exponent. Considering the value of this exponent, four cases can occur [30]:

- $0 \leq \alpha < 0.5$: the time series is stationary and contains long-range anticorrelations;
- $\alpha = 0.5$: the time series is a white noise;
- $0.5 < \alpha \leq 1$: the time series is stationary and contains long-range correlations;
- $\alpha > 1$: the time series is non-stationary.

C. Statistical analysis

Model-based predictions regarding the effect of AO-based assistance as a function of the assistance level k and the AO learning rate τ required the design of some statistics. In order to take into account the bi-linearity of the data shown in Figure 5, we fitted a linear model to the data, see (15) in the appendix. Briefly, the shape of the data can be characterized by two linear lines for each value of τ, the first one going from $k = 0$ to $k = 4$, and the second one going from $k = 4$ to $k = 20$.

Then, a general linear hypothesis test is applied on this model, using a contrast matrix allowing to compare all the conditions to the baseline with no assistance, *i.e.* $k = 0$. The p-values are also adjusted for multiple comparisons using the Benjamini & Hochberg correction. These tests are performed in R, version 3.6.2 (2019).

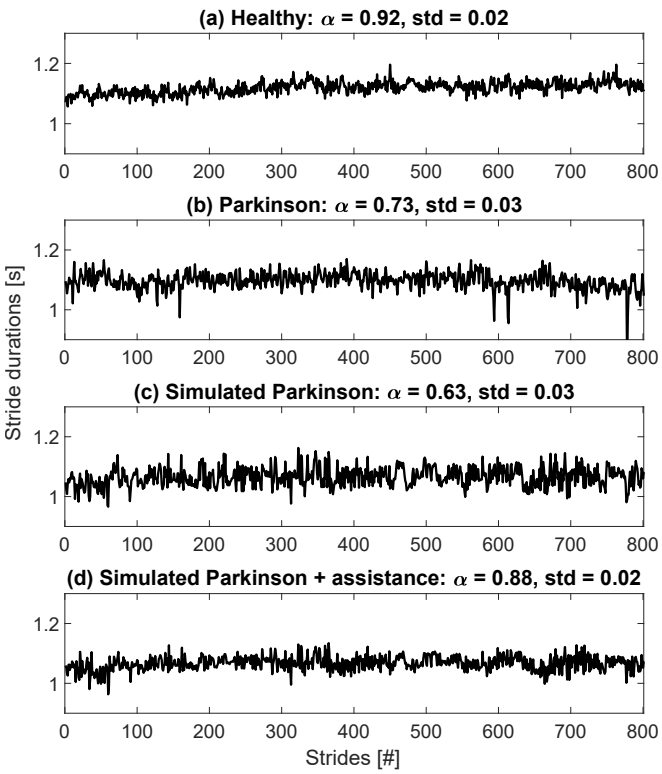

Fig. 4: Comparison between (a) a real inter-stride intervals time series of a healthy subject, from [34] and retrieved from PhysioNet; (b) a real time series of a Parkinsonian patient, from [5]; (c) a simulated time series of a Parkinsonian patient; and (d) the same simulated time series but with the AO-based assistance, with $k = 16$ and $\tau = 10$.

III. Results

A typical real time series of a healthy walker (a) and a Parkinsonian patient (b) are shown in Figure 4, as well as a simulated time series of a Parkinsonian patient, with (c) and without (d) the AO-based walking assistance. Two metrics are computed for each of them: the α exponent and the standard deviation (std). While these metrics are originally lower and higher than those of the healthy time series respectively, it can be observed that the metrics of the simulated Parkinsonian time series become closer to those of the healthy one thanks to the simulated walking assistance.

Figure 5 shows the same metrics computed for the simulated time series for different values of k and τ. In particular, it highlights an increase in α exponent and a decrease in standard deviation of the time series when k and τ increase. It also shows that for $\tau = 10$ and $k = 12$, the α exponent is close to the one of healthy walkers. Above this value, this metric is higher than 1, meaning that the time series is non-stationary, and that no conclusion can be

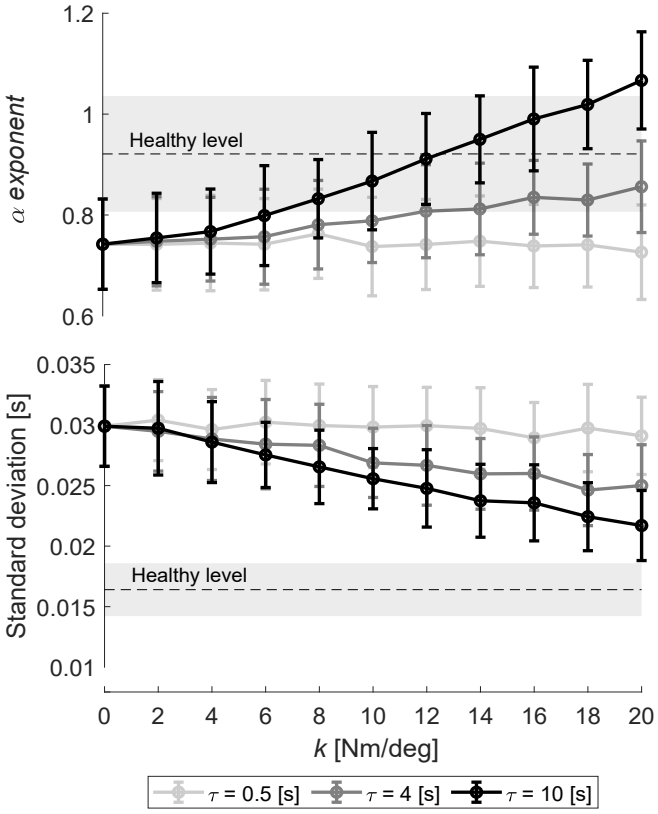

Fig. 5: Evolution of the α exponent (above) and the standard deviation (below) of the inter-stride intervals time series for several assistance levels, compared to the value of healthy walkers (means indicated by dashed lines, standard deviations indicated by shaded areas) obtained from [5]. The case where no assistance is applied corresponds to $k = 0$.

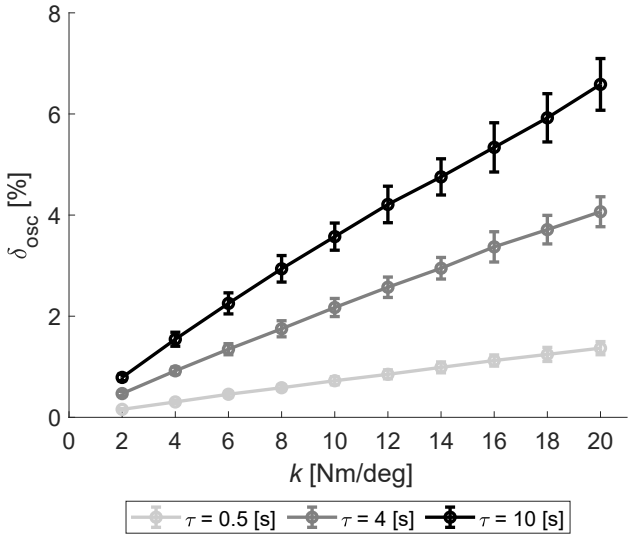

Fig. 6: Ratio δ_{osc} between the peak torque provided by the AO-based assistance and the peak total torque of the model.

drawn about its persistence. On the other hand, standard deviation of the time series becomes closer to the healthy level, but never reaches it.

With regard to the standard deviation, statistical results show that for $\tau = 0.5$, slightly significant differences between conditions were observed for $k = 16, 18, 20$ (p-value $= 0.0495, 0.0253$, and 0.0147 respectively). Highly significant differences (p-value < 0.001) were observed for $\tau = 4$ and $\tau = 10$ for all k.

Concerning the α exponent, statistics show that for $\tau = 0.5$, no significant difference can be observed between all assistance parameter pairs and baseline, while highly significant differences (p-value < 0.001) were observed for $\tau = 4$ and $k \geq 8$, and for $\tau = 10$ and $k \geq 6$.

Finally, the contribution of the torque provided by the walking assistance as a fraction of the peak total torque is provided in Figure 6. It shows that the torque contribution of the simulated AO increases with k and τ, but stays below 10% for the values we tested.

IV. Discussion

In this study, we aimed at predicting the effects of an AO-based walking assistance on the LRA of inter-stride intervals time series of Parkinsonian patients. These simulations showed that for some values of τ, great improvements can be observed for a sufficient level of assistance. We can highlight two main points from this analysis: the more k and τ increase, the more the presence of LRA in the time series increases (α exponent), and the more the variability of the time series decreases (standard deviation).

Previous articles [17], [18] have shown that AOs act as a low-pass filter on the input signal. With a higher level of assistance, the AO-based assistance filters more frequency fluctuations, and thus contributes to the decrease of the time series variability. As the time series becomes less random, the presence of LRA is increased. This particular effect of filtering out the high frequencies is visible in Figure 4, by comparing panels (c) and (d). On the other hand, the time constant τ characterizes the time it takes to the AO to learn and synchronize with the input signal. Therefore, higher values for τ means that the AO will have a longer memory, and will thus force the gait to resemble previous cycles, leading to less variability in the series.

These simulations also showed that the torque provided by the AO-based assistance was one order of magnitude smaller than the torque produced by the simulated lower limbs. Nevertheless, this assistance has a significant dynamic effect on time series metrics. This is in agreement with [35], which showed that this type of assistance had significant benefits on the harmonic content of upper-limb movement of post-stroke patients, while injecting no mechanical

work on average. These results highlight that letting the patient steering their movement without injecting too much mechanical work remains beneficial for them.

These simulations naturally lead to some assumptions and questions about the results we could obtain during actual experiments with Parkinsonian patients, who would receive this assistance with a device similar to the one pictured in Figure 1. The model predicts better results for an AO-based assistance with a longer memory, *i.e.* 10 cycles. Until now, studies that have been done with this type of walking assistance used an AO capable of learning quickly, *i.e.* about four cycles, in order to avoid preventing the user's ability to change the features of their movement. Therefore, we can ask ourselves if by using a greater learning time constant, the user will retain enough freedom to steer their movement, *i.e.* to change cadence or amplitude. In addition, the virtual stiffness k of this model must be interpreted carefully. Indeed, this value can be increased arbitrarily in this model, giving eventually rise to a normalization of the computed metrics. Nevertheless, in reality, there are physical limits to this value in order to keep the level of assistance below safety margins, so as neither harming the user nor damaging the robot. Therefore, the predictions of the model regarding the presence of LRA in the time series will probably be influenced by this limit imposed on k. Nevertheless, the model shows that the applied torque remains less than 10% of the torque produced by the lower limbs, which is within the physical limits of the actual device.

Finally, the interpretation of the parameters of the SCPG model points out a potential explanation about the origin of the loss of LRA in Parkinsonian patients. To adapt the model in order to account for the decrease in LRA in these time series, we had to decrease r_0, *i.e.* the correlation size between neural centers of a CPG. Indeed, the loss of dopaminergic neurons occurring in Parkinson's disease lead to a less correlated motor control system, modelled here through the Markov chain [36]. This decrease in LRA could also have been associated to an increase in the amplitude of the driving force of the van der Pol oscillator, as those patients pay more attention to their gait [26].

Nevertheless, this model has some limitations. It is a simplified model of the central nervous system as well as the robot. It models the loss of dopaminergic neurons by a decreased correlation between neural centers, but Parkinson's disease is much more than that. For instance, this model does not take into account the alteration of the basal ganglia pathways leading to an inhibition of the motor neurons of the cortex [37]. Moreover, it does not account for the weight of the robot, which can influence the way the user walks, by modifying the body morphology and the associated biomechanics, or by accelerating fatigue. Finally, it incorporates a model about the robot adaptation to the subject, but not the other way around.

V. Conclusion

Parkinson's disease is characterized by a loss of long-range autocorrelations in inter-stride intervals time series, and it is believed that it is an indicator of unstable gait and predictor of early falls. In contrast to first-generation assistive robots, more compliant devices like oscillator-based walking assistance allow the patient to steer their movement, potentially leading to improved gait parameters. In addition to standard gait parameters, this article predicts an improvement of the presence of LRA in the inter-stride intervals time series of Parkinsonian patients receiving an oscillator-based walking assistance with a large memory, *i.e.* about 10 cycles. Experiments are currently carried out to verify these predictions.

Appendix

A. Adaptive oscillator equations

The state-spaced dynamic equations of the AO are given by [19]:

$$\dot{\varphi}(t) = \omega(t) + \nu_\varphi \frac{F(t)}{a_1(t)} \cos(\varphi(t)) \tag{10}$$

$$\dot{\omega}(t) = \nu_\omega \frac{F(t)}{a_1(t)} \cos(\varphi(t)) \tag{11}$$

$$\dot{a}_1(t) = \eta F(t) \sin(\varphi(t)) \tag{12}$$

$$\dot{a}_0 = \eta F(t) \tag{13}$$

with the phase $\varphi(t)$, the frequency $\omega(t)$, the amplitude $a_1(t)$ and the offset $a_0(t)$.

All these variables converge to the corresponding ones of the input $x(t)$ by using as teaching signal the error between the real and estimated inputs: $F(t) = x(t) - \hat{x}(t)$.

In those equations, the learning gains are computed by [17]:

$$\eta = \frac{2}{\tau} \qquad \nu_\omega = \frac{20}{\tau^2} \qquad \nu_\varphi = \sqrt{24.2\nu_\omega} \tag{14}$$

where η is the integrator gain, ν_ω is the frequency gain, ν_φ is the phase gain, and τ is a time constant determining the time for the oscillator to learn the input signal features.

B. Statistical linear model equation

The bilinear model used to fit the shape of the data in Figure 5 is given by:

$$\begin{aligned} H_{i,k,\tau} = {} & \beta_0 + \beta_1\, k + \beta_2\, k\, \mathbb{1}_{\tau=4} + \beta_3\, k\, \mathbb{1}_{\tau=10} \\ & + \beta_4\, \max(k-4,0) + \beta_5\, \max(k-4,0)\, \mathbb{1}_{\tau=4} \\ & + \beta_6\, \max(k-4,0)\, \mathbb{1}_{\tau=10} + \varepsilon_{i,k,\tau} \end{aligned} \tag{15}$$

for $i = 1, 2, ..., 10$ and $k = 0, 2, ..., 20$.

In this equation, H is the answer variable, *i.e.* the α exponent or the standard deviation of the inter-stride intervals time series, β_0 is the ordinate at the origin for $k = 0$, $\mathbb{1}_{\tau=t}$ is the indicator function, *i.e.* it is equal to 1 if

$\tau = t$ and to 0 if $\tau \neq t$, and $\varepsilon_{i,k,\tau} \sim \mathcal{N}(0, \sigma_\varepsilon^2)$ is the error term.

A first line is fitted for each τ to the data between $k = 0$ and $k = 4$, and is characterized by the slope β_1 for $\tau = 0.5$, β_2 for $\tau = 4$, and β_3 for $\tau = 10$. Then a second line is fitted to the data between $k = 4$ and $k = 20$, and is characterized by the slope β_4 for $\tau = 0.5$, β_5 for $\tau = 4$, and β_6 for $\tau = 10$.

VI. Acknowledgement

We thank Alexandre Jacquemain (UCLouvain) for his great help in the statistical analysis.

References

[1] Parkinson's Foundation, "Understanding Parkinson - Statistics," [online] https://www.parkinson.org/Understanding-Parkinsons/Statistics, consulted in June 2021.

[2] A. Zanardi et al., "Gait parameters of Parkinson's disease compared with healthy controls: a systematic review and meta-analysis," Scientific Reports, vol. 11, 2021.

[3] Parkinson's Foundation, "Movement Symptoms - Trouble Moving or Walking," [online] https://www.parkinson.org/Understanding-Parkinsons/Symptoms/Movement-Symptoms/Trouble-Moving-or-Walking, consulted in June 2021.

[4] L. Kalilani, M. Asgharnejad, T. Palokangas, and T. Durgin, "Comparing the incidence of falls/fractures in Parkinson's disease patients in the US population," PLoS One, vol. 11, no. 9, 2016.

[5] T. Warlop et al., "Temporal organization of stride duration variability as a marker of gait instability in Parkinson's disease," J. Rehabil. Med., vol. 48, no. 10, pp. 865–871, 2016.

[6] T. Warlop, B. Bollens, F. Crevecoeur, C. Detrembleur, and T. Lejeune, "Dynamics of revolution time variability in cycling pattern: voluntary intent can alter the long-range autocorrelation," Annals of Biomedical Engineering, vol. 41, no. 8, pp. 1604-1612, 2013.

[7] V. Marmelat and D. Delignières, "Complexity, coordination, and health: avoiding pitfalls and erroneous interpretations in fractal analyses," Medicina (Kaunas), vol. 47, no. 7, pp. 393-398, 2011.

[8] F. Giovacchini et al., "A light-weight active orthosis for hip movement assistance," Robotics and Autonomous Systems, vol. 73, pp. 123-134, 2015.

[9] R. Bartsch, M. Plotnik, J. Kantelhardt, S. Havlin, N. Giladi, and J. Hausdorff, "Fluctuation and synchronization of gait intervals and gait force profiles distinguish stages of Parkinson's disease," Physica A., vol. 383, no. 2, pp. 455-465, 2007.

[10] J. Hausdorff, "Gait dynamics in Parkinson's disease: Common and distinct behavior among stride length, gait variability, and fractal-like scaling," CHAOS, vol. 19, 2009.

[11] A. Picelli et al., "Robot-assisted gait training in patients with parkinson disease: A randomized controlled trial," Neurorehabilitation and Neural Repair, vol. 26, no. 4, pp. 353-361, 2012.

[12] A. Lo, V. Chang, M. Gianfrancesco, J. Friedman, T. Patterson, and D. Benedicto, "Reduction of freezing of gait in Parkinson's disease by repetitive robot-assisted treadmill training: A pilot study," Journal of NeuroEngineering and Rehabilitation, vol. 7, no. 1, 2010.

[13] S. J. Yun, H. H. Lee, W. H. Lee, S. H. Lee, B.-M. Oh, and H. G. Seo, "Effect of robot-assisted gait training on gait automaticiy in Parkinson disease," Medicine, vol. 100, no. 5, 2021.

[14] M. Capecci et al., "Clinical effects of robot-assisted gait training and treadmill training for Parkinson's disease. A randomized controlled trial," Annals of Physical and Rehabilitation Medicine, vol. 62, no. 5, pp. 303-3012, 2019.

[15] N. Hoban et al., "Motions or muscles? Some behavioral factors underlying robotic assistance of motor recovery," JRRD, vol. 43, no. 5, pp. 605-618, 2006.

[16] H. Vallery, J. Veneman, E. van Asseldonk, R. Ekkelenkamp, M. Buss, and H. van der Kooij, "Compliant actuation of rehabilitation robots," IEEE Robotics & Automation Magazine, vol. 15, no. 3, pp. 60-69, 2008.

[17] R. Ronsse, S. De Rossi, N. Vitiello, T. Lenzi, M. Carrozza, and A. Ijspeert, "Real-time estimate of velocity and acceleration of quasi-periodic signals using adaptive oscillators," IEEE, vol. 29, no. 3, pp. 783-791, 2013.

[18] R. Ronsse, N. Vitiello, T. Lenzi, J. van den Kieboom, M. Carrozza, and A. Ijspeert, "Human-robot synchrony: flexible assistance using adaptive oscillators," IEEE Transactions on Biomedical Engineering, vol. 58, no. 4, pp. 1001-1012, 2010.

[19] R. Ronsse et al., "Oscillator-based assistance of cyclical movements: model-based and model-free approaches," Medical & Biological Engineering & Computing, vol. 49, 2011.

[20] P. Leconte and R. Ronsse, "Performance-based robotic assistance during rhythmic arm exercises," Journal of NeuroEngineering and Rehabilitation, vol. 13, no. 82, 2016.

[21] V. Ruiz Garate et al., "Experimental validation of motor primitive-based control for leg exoskeletons during continuous multi-locomotion tasks," Front. Neurorobot., vol. 11, 2017.

[22] K. Seo, S. Y. Hyung, B. K. Choi, Y. Lee, and Y. Shim, "A new adaptive frequency oscillator for gait assistance," IEEE ICRA, pp. 5565-5571, 2015.

[23] K. Seo, J. Lee, Y. Lee, T. Ha, and Y. Shim, "Fully autonomous hip exoskeleton saves metabolic cost of walking," IEEE ICRA, pp. 4628-4635, 2016.

[24] Cyberlegs++, [online] http://www.cyberlegs.eu/.

[25] E. Martini et al., "Gait training using a robotic hip exoskeleton improves metabolic gait efficiency in the elderly," Sci. Rep., vol. 9, no. 1, 2019.

[26] B. West and N. Scafetta, "Nonlinear dynamical model of human gait," Physical Review E, vol. 67, no. 5, 2003.

[27] D. Delignières and K. Torre, "Fractal dynamics of human gait: a reassessment of the 1996 data of Hausdorff et al.," J. Appl. Physiol., vol. 106, no. 4, pp. 1272-1279, 2009.

[28] Y. Ashkenazy, J. Hausdorff, P. Ivanov, and H. Stanley, "A stochastic model of human gait dynamics," Physica A: Statistical Mechanics and its Applications, vol. 316, pp. 662-670, 2002.

[29] G. Rangarajan and M. Ding, "Integrated approach to the assessment of long range correlation in time series data," Physical Review E, vol. 61, no. 5, pp. 4991-5001, 2000.

[30] C. Roume, "La complexité du mouvement humain : aspects théoriques et pratiques de l'évaluation et de l'interaction des complexités au service de la réhabilitation," PhD thesis, Université de Montpellier, 2019.

[31] Z. Almurad and D. Delignières, "Evenly spacing in Detrended Fluctuation Analysis," Physica A, vol. 451, pp. 63-69, 2016.

[32] V. Marmelat, N. Reynolds, and A. Hellman, "Gait dynamics in Parkinson's disease: short gait trials "stitched" together provide different fractal fluctuations compared to longer trials," Frontiers in Physiology, vol. 9, 2018.

[33] B. Mandelbrot and J. Van Ness, "Fractional brownian motions, fractional noises and applications," SIAM Review, vol. 10, no. 4, pp. 422-437, 1968.

[34] J. Hausdorff, P. Purdon, C.-K. Peng, Z. Ladin, J. Wei, and A. Goldberger, "Fractal dynamics of human gait: stability of long-range correlations in stride interval fluctuations," J. Appl. Physiol., vol. 80, no. 5, pp. 1448-1457, 1996.

[35] P. Leconte, G. Stoquart, T. Lejeune, and R. Ronsse, "Rhythmic robotic training enhances motor skills of both rhythmic and discrete upper-limb movements after stroke: a longitudinal pilot study," International Journal of Rehabilitation Research, vol. 42, no. 1, pp. 46-55, 2019.

[36] N. Scafetta, D. Marchi, and B. West, "Understanding the complexity of human gait dynamics," CHAOS, vol. 19, no. 2, 2009.

[37] M.-P. Laplante Campbell, "Caractérisation de modèles murins de la maladie de Parkinson (MPTP, PITX3) et modification des cellules souches hématopoïetiques pour stimuler la production du « brain-derived neurotrophic factor » (BDNF)," PhD thesis, Université Laval, 2008.